horticulturae

MDPI

Article

Genome-Wide Identification of MYB Transcription Factors and Their Function on Floral Volatile Compounds Biosynthesis in *Antirrhinum majus* L.

Xiaohui Song †, Senbao Shi †, Yulai Kong, Fengyi Wang, Shaorong Dong, Chong Ma, Longqing Chen * and Zhenglin Qiao *

Yunnan Province Engineering Research Center for Functional Flower Resources and Industrialization, College of Landscape Architecture and Horticulture Sciences, Southwest Forestry University, Kunming 650024, China; songxh@swfu.edu.cn (X.S.); shisb@swfu.edu.cn (S.S.); kongyulai@swfu.edu.cn (Y.K.); wangfengyi@swfu.edu.cn (F.W.); dongshaorong0130@126.com (S.D.); machong202312@163.com (C.M.)

* Correspondence: chenlq@swfu.edu.cn (L.C.); qiaozl@swfu.edu.cn (Z.Q.); Tel.: +86-0871-63862842 (Z.Q.)

† These authors contributed equally to this work.

Abstract: The v-MYB avivan myoblastsis virus oncogene homolog (MYB) family is the largest gene family of the transcription factor in plants, involved in plant growth and development, secondary metabolism and resistance to biotic/abiotic stress. *Antirrhinum majus* (snapdragon) is an ideal material for studying ornamental traits. Nevertheless, there has been no systematic investigation into the *AmMYB* family of snapdragons. In this study, we identified a total of 162 members of the *AmMYB* gene family in snapdragons. Gene structure analysis showed that the AmMYB family within the same subgroup had a similar structure and motifs. Analysis of gene duplication events revealed that the amplification of the *AmMYB* family was driven by whole-genome duplication (WGD) and dispersed duplication. The analysis of cis-acting elements in the promoter region of *AmMYB* genes reveals a collaborative involvement of light-responsive growth and development elements, stress resistance elements, and hormone-responsive elements jointly participating in the regulation of the *AmMYB* gene. Collinearity analysis demonstrates significant functional distinctions between *AmMYB* and monocotyledonous plants. The classification of *AmMYB* members results in 3 main subgroups with 36 smaller subgroups. All *AmMYB* genes are distributed across all eight chromosomes, with no apparent correlation between subfamily distribution and chromosome length. Through phylogenetic analysis and RNA-seq analysis, we have identified 9 *R2R3-MYB* genes that potentially play a role in the regulation of floral volatile organic compounds (FVOCs) biosynthesis. Their expression patterns were verified by qRT-PCR experiments. This study establishes a robust foundation for further investigations into the functionality of *AmMYB* genes and their molecular mechanisms underlying FVOC biosynthesis in snapdragons.

Keywords: MYB transcription factors; genome-wide identification; *Antirrhinum majus*; gene expression; floral volatile organic compounds (FVOCs)

check for updates

Citation: Song, X.; Shi, S.; Kong, Y.; Wang, F.; Dong, S.; Ma, C.; Chen, L.; Qiao, Z. Genome-Wide Identification of MYB Transcription Factors and Their Function on Floral Volatile Compounds Biosynthesis in *Antirrhinum majus* L. *Horticulturae* **2024**, *10*, 136. https://doi.org/10.3390/horticulturae10020136

Academic Editor: Haiying Liang

Received: 20 December 2023
Revised: 13 January 2024
Accepted: 23 January 2024
Published: 30 January 2024

Copyright: © 2024 by the authors. Licensee MDPI, Basel, Switzerland. This article is an open access article distributed under the terms and conditions of the Creative Commons Attribution (CC BY) license (https://creativecommons.org/licenses/by/4.0/).

1. Introduction

Transcription factors (TFs) play a pivotal role in the regulation of plant physiological and biochemical processes, exerting significant influence on species evolution through self-regulation or downstream target gene transcription [1]. TFs are typically composed of multiple functionally independent binding domains, which categorize them into different families based on these domains [2,3]. The v-MYB avivan myoblastsis virus oncogene homolog (MYB) TFs family is the largest TFs family in plants working in plant growth and development, secondary metabolism and resistance to biotic and abiotic stress [4–7]. The first *MYB* was identified in the avian myoblast virus, and the first plant *MYB* was isolated

from *Zea mays* [8,9]. Subsequently, researchers have continuously identified and elucidated the biological functions of *MYB* family members across various species [10–12].

The distinguishing feature of MYB TFs lies in the presence of a highly conserved DNA binding domain in the N-terminus, which comprises one or more repeat (R) structures [13,14]. Each R structure is characterized by three relatively conserved tryptophans that form a helix–turn–helix (HTH) motif, facilitating the binding to the target gene. Additionally, they also contain several α-helices encoded by 50–53 amino acids at the N-terminus [15]. The second and third α-helices possess the ability to bind to specific DNA sequence motifs, thereby activating the expression of target genes [16]. According to the number of repetitions, plant MYB TFs can be classified into four types: 1R-MYB, R2R3-MYB, 3R-MYB, and 4R-MYB [4,17]. The class of 1R-MYB proteins plays a crucial role as telomere-binding proteins in maintaining chromosome structure integrity and regulating gene transcription [18,19]. The family of the 1R-MYB proteins has been categorized into five subfamilies: I-box-binding like, CPC like, CCA1 like, R-R like and TBP like [20]. In comparison with the *R2R3-MYB* genes, these *MYB*-related genes have received limited attention with only a few studies conducted on their functions. The *CCA1-like* gene is involved in circadian rhythm maintenance [21,22]. The *CPC-like* gene is involved in the regulation of cellular morphogenesis. In *Arabidopsis thaliana*, a specific *CPC-like* gene encodes a small protein containing a MYB domain but lacking a transcriptional activation domain, which plays a role in trichome and root hair development [23,24]. R1R2R3-MYB primarily participates in cell cycle control and cell differentiation regulation. Currently, the number of identified 4R-MYB subfamilies in plants remains limited (Supplementary Table S1).

R2R3-MYB contains two conserved R2 and R3 repeat sequences, as well as a regulatory domain (activation or inhibition function) within the C-terminus variable region. It has numerous members and diverse functions [19]. There has been controversy regarding the order of appearance of R2R3-MYB, with one faction positing that R1R2R3-MYB is formed through the absence of R1. Conversely, the opposing viewpoint suggests that it is formed through the repetition of R1 in 1R-MYB [20,25]. Based on the conservation of the DNA binding domain and amino acid motifs in the C terminal domains, subgroups have been established for R2R3-MYB proteins [4]. In Arabidopsis, the *AtMYB* genes encode R2R3-type MYB factors, which have been classified into 22 subgroups [17].

In the *MYB* family, R2R3-MYB TFs are predominantly abundant in plants [26]. Members of R2R3-MYB are involved in plant stress resistance and regulating synthesis in secondary metabolic pathways in various plant species including Arabidopsis, grapes, apples, and Petunia [27–33]. AtMYBL2 has been proven to inhibit the production of anthocyanins in *A. thaliana* [34]. Similarly, the grape *VvMYB4-like* gene and the soybean *GmMYB100* can negatively regulate the biosynthesis of plant flavonoids [35,36]. MdMYB3 can bind with downstream structural genes of the apple flavonoid metabolism pathway to regulate anthocyanin synthesis [37]. Research has found that the MBW ternary complex composed of R2R3-MYB, bHLH TFs and WD40 protein is an important substance for activating core enzymes or genes in the flavonoid and anthocyanin pathways [38,39]. For example, the interaction between strawberry *FaEGL3* and *FaLWD1/FaLWD1-like* with R2R3-FaMYB5 positively regulates the biosynthesis of anthocyanins and proanthocyanins [40].

In addition to regulating the metabolic pathways of flavonoids and anthocyanins, the R2R3-MYB TFs also have a significant impact on floral fragrance synthesis. Research has shown that the transcription inhibitor MYB controls carbon flow distribution by acting on *C4H*, thereby affecting the synthesis pathways of volatile phenylpropanoids, including eugenol and isoeugenol. After silencing *PhMYB4*, the transcription levels of the *PhC4H* gene in *Petunia hybrida* significantly increase [41]. ODORANT1 (ODO1) is the first R2R3 type MYB TFs discovered in Petunia [42], ODO1, BENZENOID II (EOBII), EOBI and LATE ELONGATED HYPOCOTYL (LHY) regulate the odor production of flowers by activating odor related genes in *P. hybrida* [43,44]. FaMYB10 and FaEOBII in *Fragaria* × *ananassa* participate in the regulation of eugenol [6,45]. Overexpression of *SmMYB39* alters the synthesis of rosmarinic acid by inhibiting *C4H* and tyrosine aminotransferase genes, reducing the

content of 4-coumaric acid, rosmarinic acid, and other substances. When *SmMYB39* is silenced by RNAi, the content of these compounds increases [46]. In addition, multiple R2R3-MYB pathways regulating terpene-related pathways have been identified [47,48]. *MYB44* negatively regulates citral biosynthesis by directly binding to the promoter of the *ADH* coding gene [49]. In *Freesia hybrida*, FhMYB21L2 directly activates the expression of terpene synthase *FhTPS1* by binding to the MYBCORE site in the *FhTPS1* promoter [47]. The biosynthesis of terpenoid volatiles in *Hedychium coronarium* is regulated by MYB and ARF5 TFs [3,50,51].

Antirrhinum majus (snapdragon) is a perennial, erect herbaceous plant belonging to the Plantaginaceae family. It is highly valued as an ornamental flower and extensively utilized in landscape architecture and as a cut flower, as well as being a pivotal model plant [52]. The floral volatiles of snapdragons are mainly composed of a combination of floral volatile terpenoids (FVTs), floral volatile phenylpropanoids/benzenoids (FVPBs) and floral volatile fatty acid derivatives (FFADs) [53]. For example, limonene, laurylene, linalool, benzaldehyde, methyl salicylate, benzyl alcohol, acetophenone, phenylethanol and basilene. Among them, FVTs are the most abundant floral volatiles in snapdragons [54]. Methylbenzoate is one of the most abundant odor compounds detected in most *A. majus* cultivars [55]. These volatile compounds are important biological characteristics of plants, with functions such as attracting pollinators, serving as biological signals for the plant body to sense external stimuli, and participating in biological and abiotic stress responses [56]. The release amount and compound types of FVOCs may vary depending on the variety of snapdragon, as well as different flowering stages. They may also vary with different light conditions, temperatures, or circadian rhythms [44,57]. Myrcene was present in the scent of *A. majus* 165E and acetophenone was the most abundant FVOC produced by *A. majus* Sippe50. *A. linkianum*, *A. tortuosum* and *A. braun-blanquetii* emit the most ocimene. *A. graniticum* releases the most cinnamyl alcohol [53].

Despite extensive exploration of some *AmMYB* family members in snapdragons [58–65], little is known about the entire *AmMYB* family evolution history and functional analyses in *A. majus*. In this study, we identified all the *AmMYB* gene family members from the *A. majus* whole genome data. We conducted a comprehensive investigation of the family including *AmMYB* gene structure, chromosome localization, phylogenetic relationships, motif composition, cis-element composition and expression patterns of *AmMYB* genes to obtain an extensive and comprehensive understanding of the *AmMYB* family in snapdragons.

2. Materials and Methods

2.1. Plant Materials and Growth Conditions

Two dwarf varieties of *Antirrhinum majus* were used in the study: '*Floral Showers White*' and '*Floral Showers Red Pink*'. The plants were planted in a greenhouse at the Southwest Forestry University experimental base in Kunming, Yunnan province, China (longitude: 102.76°; latitude: 25.06°). Sowed on 10 July 2023, in a 32-hole tray (560 mm) containing seedling soil × two hundred and eighty × 53mm, transplanted to PP plastic pots (upper diameter 150 mm, lower diameter 125 mm, height 165 mm) on 20 August of the same year, with a pot soil ratio of 3:2:1 for garden soil/ planting soil/perlite. After transplanting to the planting pot, compound fertilizer should be applied once a month, with normal watering management. The plant grows under natural light and temperature conditions of 20–25 °C, and the flowering period begins in October of the same year. On sunny days with sufficient sunlight and suitable temperature, harvest the flowers (bud stage: FB; petal stage: A1; initial flowering stage: A2; full flowering stage: A3; final flowering stage: A4), immediately freeze leaves, stems, roots, and other tissues with liquid nitrogen, and then store at −80 °C.

2.2. Whole Gene Identification and Physicochemical Property Analysis of the AmMYB Transcription Factor Family in Snapdragons

The snapdragon genome and annotation files were downloaded from the Snapdragon Genome Database database (http://bioinfo.sibs.ac.cn/Am/, accessed on 1 October 2023).

Perform a bidirectional Blast using the protein sequences of the *Arabidopsis MYB* family and snapdragon to screen for potential members of the *AmMYB* gene family MYB ($E \leq 1 \times 10^{-5}$). Simultaneously, retrieve the conserved MYB domain (PF00249) from the Pfam database, use NCBI-CDD (https://www.ncbi.nlm.nih.gov/, accessed on 3 October 2023) to search for the MYB conservative domain ($E \leq 1 \times 10^{-5}$), delete redundant sequences, and finally use SMART to further check the integrity of the conservative sequence. Name the *AmMYB* candidate gene *AmMYB1* to *AmMYB162* based on its position on the chromosome. Online analysis of the physicochemical properties of AmMYB protein, such as molecular weight, isoelectric point, instability coefficient, etc., using the Expasy database (SIB Swiss Institute of Bioinformatics | Expasy). Use online software WoLF PSORT (https://wolfpsort.hgc.jp/, accessed on 3 October 2023) tools for subcellular localization prediction [66].

2.3. Conservative Motif and Gene Structure Analysis of AmMYB Transcription Factor Protein

Using the online software MEME (https://meme-suite.org/meme/, accessed on 7 October 2023) to perform conserved motif analysis on AmMYB proteins. The TBtools software v2.028 built-in function (gene structure view) was used to visualize the gene structure (UTR/exon/intron) simultaneously [67].

2.4. Chromosomal Localization and Replication Event Analysis of AmMYB Transcription Factors

The physical location of the *AmMYB* genes (Gene Location Visualize), tandem replication and fragment replication events can be determined by utilizing GFF files and genome sequence files, *MYB* and visualized with TBtools.

2.5. AmMYB Transcription Factor Multiple Sequence Alignment and Phylogenesis

AtMYB protein sequence was downloaded from the Tair website (https://www.arabidopsis.org/, accessed on 1 October 2023), and Cluster W in MEGA-X software was used to perform multi-sequence alignment of AtMYB and AmMYB protein sequences [68]. The phylogenetic tree was constructed using the Neighbor-joining Method (NJ), with Jones Taylor Thornton (JTT) model, partial deletion of Gap, and Bootstrap method of 1000. The online Itol (https://itol.embl.de/, accessed on 7 October 2023) was used to beautify the phylogenetic tree.

2.6. Analysis of AmMYB Transcription Factor Promoter

We used TBtools to extract 2000 bp upstream of the *AmMYB* gene start codon (ATG) as the promoter sequence (Gtf/Gff3 Sequences Extract) from snapdragon genome data. And the cis-acting elements of the *AmMYB* gene promoter region were analyzed using the online software PlantCare (https://www.ugent.be/, accessed on 2 October 2023) [69].

2.7. Analysis of Intra and Inter-Species Collinearity of AmMYB Transcription Factors

Replication events within and between species were evaluated using TBtools software MCS canX (version 2.041). The genome files of rice, tomato, potato, and *Arabidopsis* are from the National Center for Biotechnology Information website (https://www.ncbi.nlm.nih.gov/, accessed on 1 October 2023).

2.8. Transcriptome Sequencing Analysis

The transcriptome data of five flowering stages of Corolla (FB, A1, A2, A3, A4) from Am13 and Am15 were downloaded from NCBI (BioProject ID: SUB13300760). The task involves identifying candidate genes in transcriptome data based on FPKM (Fragments Per Kilobase Per Million mapped reads) values and generating a heatmap visualization using TBtools.

2.9. RNA Extraction and qRT-PCR Analysis

We extracted RNA from five flowering stages of snapdragons using the rapid RNA extraction kit from Beijing Adlai Biotechnology Company. Using the M-MLV4 first-

strand cDNA Synthesis Kit from BoMed Biotech, the first-strand cDNA was synthesized using RNA as a template. We designed qRT-PCR primers using Premier 5 software (Supplementary Table S2). We selected the snapdragon ubiquitin gene (*AmUBI*) as the internal reference gene [70]. The qRT-PCR was conducted following the abm® BlasTaqTM 2 × qPCR Master Mix Kit instructions, each with three biological replicates. The relative expression level of genes is $2^{-\Delta\Delta CT}$ calculation [71].

3. Results

3.1. Characterization and Identification of AmMYB Genes in Snapdragon Genome

In order to identify members of the *AmMYB* gene family, a total of 162 *AmMYB* genes were identified through bidirectional blast alignment of *AtMYB* members. These genes were named *AmMYB1* to *AmMYB162* based on the position of the chromosomes (Supplementary Table S3). Subsequently, an analysis was conducted on the open reading frames (ORF), amino acid length (AA), molecular weight (MW), theoretical isoelectric point (pI), protein stability coefficient (Ii), fat coefficient and protein hydrophobicity of these 162 *AmMYB* genes. The AmMYB protein exhibits an open reading frame spanning from 231 bp~3225 bp, with an amino acid length ranging from 76 aa~1074 aa. Notably, there is a significant difference in protein molecular weight, ranging from 8.65 kDa to 119.64 kDa. The theoretical isoelectric point is within the range of 4.6 and 10.38, while the instability coefficient varies between 30.39 and 75.41. Among these proteins, a total of 153 are classified as unstable proteins, leaving only 9 that can be considered stable proteins. All identified proteins exhibit hydrophilic characteristics with hydrophilicity and hydrophobicity index values ranging from −1.286 to −0.318. The subcellular localization prediction results revealed that, with the exception of AmMYB26 being localized in the cytoplasm, AmMYB51 in the mitochondria, and AmMYB112 and AmMYB160 in the chloroplasts, all other proteins were predominantly localized within the nucleus.

3.2. Genes Structure and Conserved Motifs of AmMYB Genes

To understand the structure of the *AmMYB* genes, an analysis was conducted on the intron–exon relationship of the *AmMYB* genes (Figure 1). A phylogenetic tree was constructed based on the protein sequences of 162 AmMYB proteins, which were classified into three subfamilies. The number of exons in the *AmMYB* genes ranged from 1 to 8, with a minimum of 1 exon observed in 5 genes and a maximum of 108 exons found in 3 genes. Most *AmMYB* genes exhibited 2 or 3 exons. Notably, closely clustered *AmMYB* genes shared similar exon–intron structures, particularly regarding exon length and quantity.

The MEME online software was utilized to predict conserved motifs of the 162 AmMYB proteins, as depicted in Figure 2. We found 15 conserved (Supplementary Table S4). The analysis of the 15 conserved motifs showed that motif 2 appeared the most frequently, with a total of 162 occurrences. It appeared once in each AmMYB protein sequence and was distributed at the N-terminus of the MYB protein. The motif 14 appears the least frequently, only 4 times, respectively, near the C-terminus of AmMYB130, AmMYB131, AmMYB132, and AmMYB133. In terms of the number of motifs, AmMYB75 exhibits the lowest number of motifs, with only motif 2 being present. On the other hand, AmMYB128 displays the highest number of motifs, with a total of 9 conserved motifs observed. With the exception of motif 4, motif 2, motif 3, and motif 1 appearing once, motif 11 appears twice, motif 15 appears 3 times, and motif 15 appears near the C-terminus, repeating its appearance. Although the motifs between different clusters are not exactly the same, AmMYB proteins within the same cluster usually have similar motifs, suggesting that the phylogenetic model of AmMYB proteins may be influenced by motif positions.

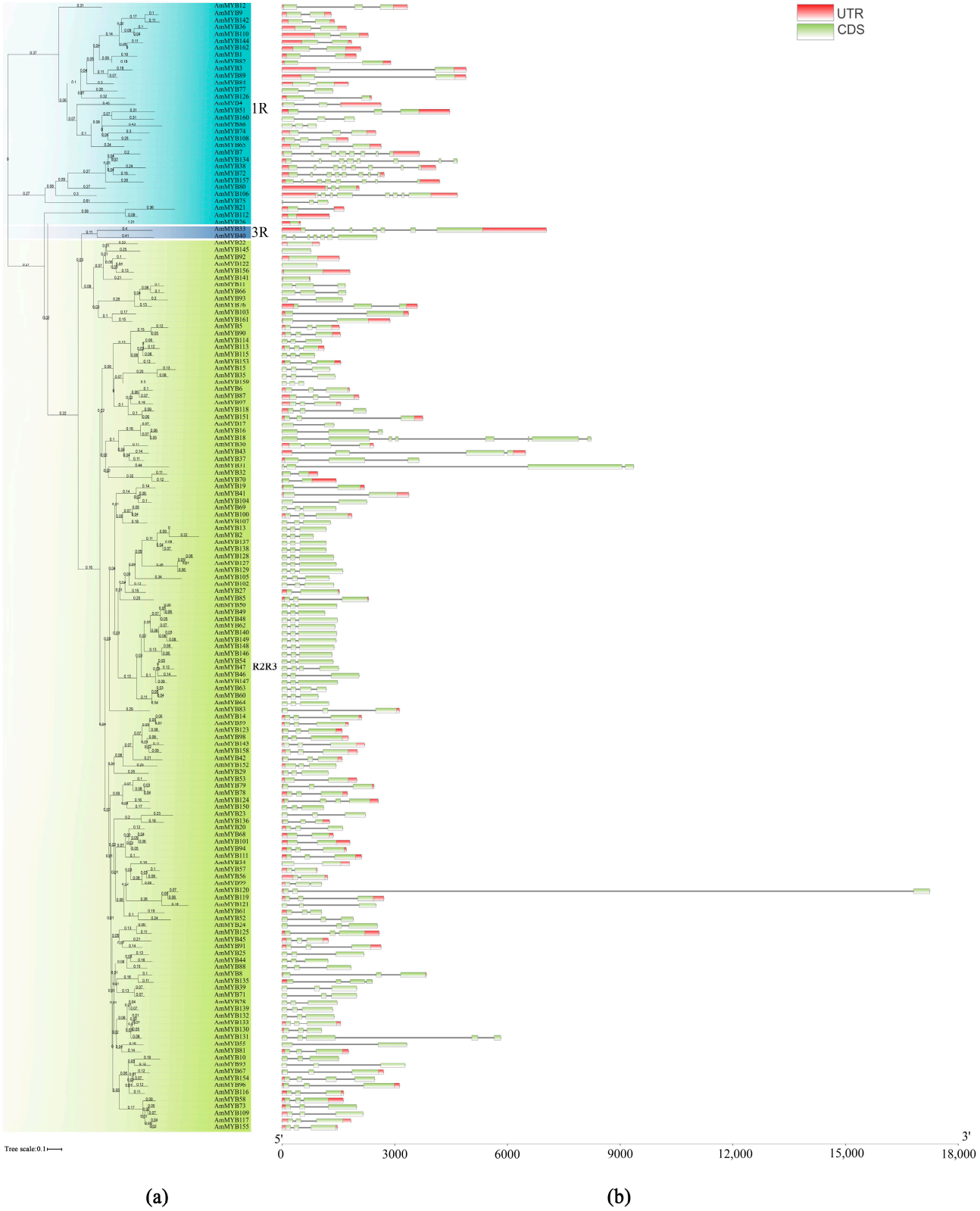


Figure 1. Gene structure and evolution of *AmMYB* family in *A. majus*. (**a**) Phylogenetic relationships of AmMYB. Three subfamilies are represented by three different colors; (**b**) intron–exon structure of bottom demonstrates the length of exons and introns.

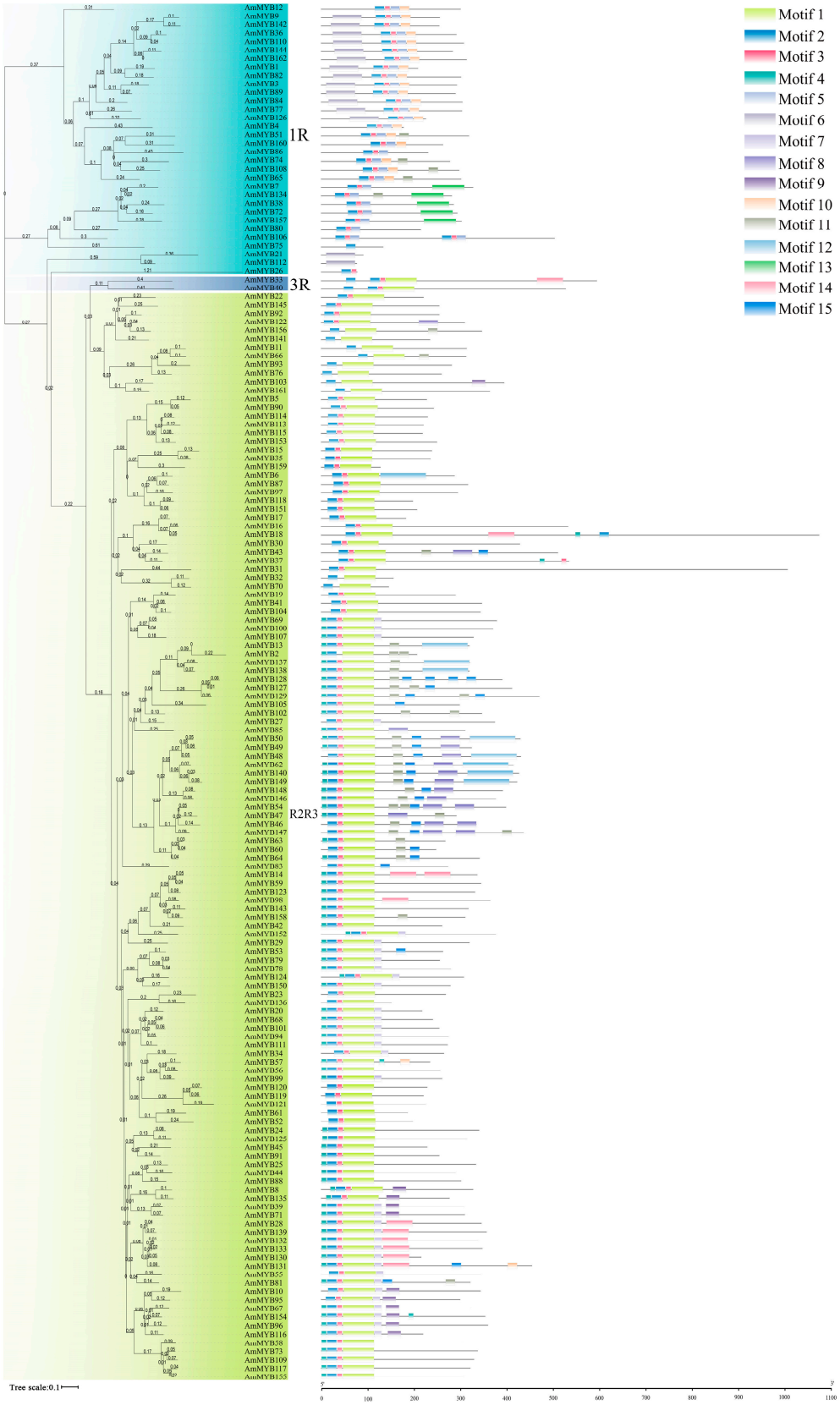


Figure 2. Conserved motifs for AmMYB proteins in *A. majus*. Different motifs are shown with different colored boxes. The gray lines represent the non-conserved sequences. The lengths of motifs can be estimated using the scale at the bottom.

3.3. Phylogenetic Analysis of the AmMYB Gene Family

The potential evolutionary relationship of AmMYB TFs was investigated by constructing a phylogenetic tree using MEGA-X software (version 11.0.10), comparing the AmMYB protein with the *Arabidopsis* MYB protein (Figure 3). The phylogeny analysis revealed that AmMYB members can be classified into three subfamilies, namely 1R-AmMYB, R2R3-AmMYB, and R3-AmMYB. Among these subfamilies, R2R3-AmMYB has the highest representation at 79.01%, while 3R-AmMYB has the lowest representation at only 1.23%. Additionally, 1R-AmMYB accounts for 19.75% of the total members. Subsequently, the 3 subfamilies were further classified into 36 subfamilies, comprising 5 subfamilies for 1R-AmMYB, 30 subfamilies for R2R3-AmMYB, and only 1 subfamily for R3-AmMYB. In the evolutionary tree, with the exception of S5, S12, S15, and TBP-like subfamilies, all amino acid sequences of AmMYB could be clustered with the *Arabidopsis* AtMYB subfamily. This suggests that the evolution of the AmMYB gene is relatively conserved and exhibits high homology with the AtMYB family. It can be speculated that AmMYB shares certain functional similarities with the AtMYB family.

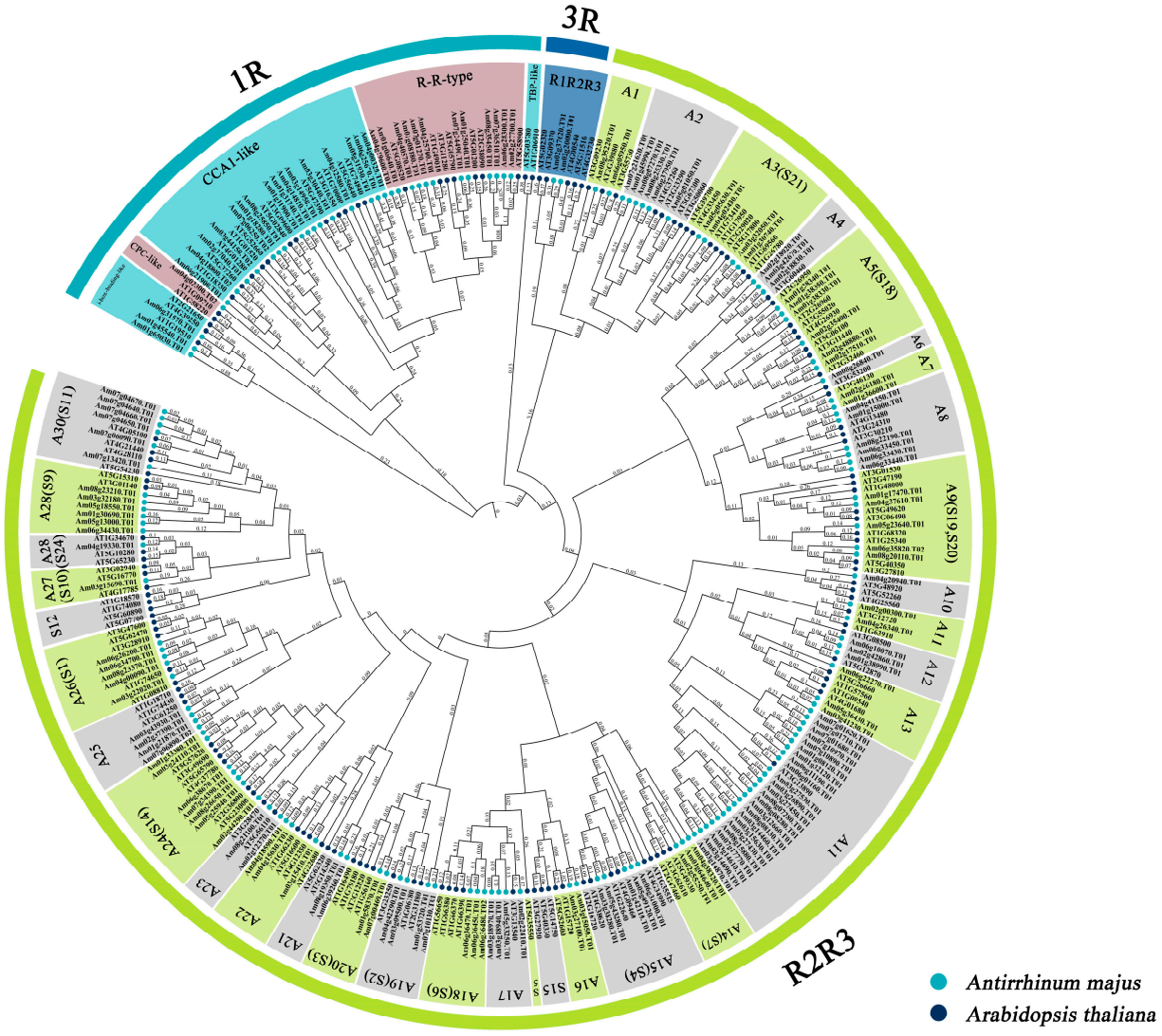


Figure 3. Phylogenetic analysis of MYB proteins from *A. majus* L. and *A. thaliana*. Dark blue circles represent *Arabidopsis* MYB members, light blue circles represent snapdragonMYB members; different color arcs represent MYB subfamily classification; groups were identified according to the subfamilies in *Arabidopsis*.

3.4. Chromosomal Localization of AmMYB Genes

The chromosomal localization information of *AmMYB* gene family members was determined using the snapdragon gene annotation file (Figure 4). As depicted in Figure 3, the distribution of *AmMYB* genes spans across all eight chromosomes. Among them, chromosome 1 harbors 26 *AmMYB* genes, chromosome 2 contains 18 *AmMYB* genes, chromosome 3 possesses 8 *AmMYB* genes, chromosome 4 encompasses 19 *AmMYB* genes, chromosome 5 accommodates 10 *AmMYB* genes, chromosome 6 houses 23 *AmMYB* genes, chromosome 7 contains 20 *AmMYB* genes and chromosome 8 has 18 *AmMYB* genes. From the perspective of subfamily classification, *1R-AmMYB* is distributed except for chromosome 5, it is predominantly concentrated on chromosomes 1 and 4, with a total of 8 *AmMYB* genes present, while the distribution of the *3R-AmMYB* subfamily is limited to chromosome 2 only. The lengths of chromosomes 1 to 8 are 71.72 Mb, 75.46 Mb, 62.72 Mb, 50.91 Mb, 71.57 Mb, 55.04 Mb, 52.49 Mb and 57.08 Mb, respectively. These findings suggest that the distribution pattern of different *AmMYB* subfamily members does not necessarily correlate with chromosome length.

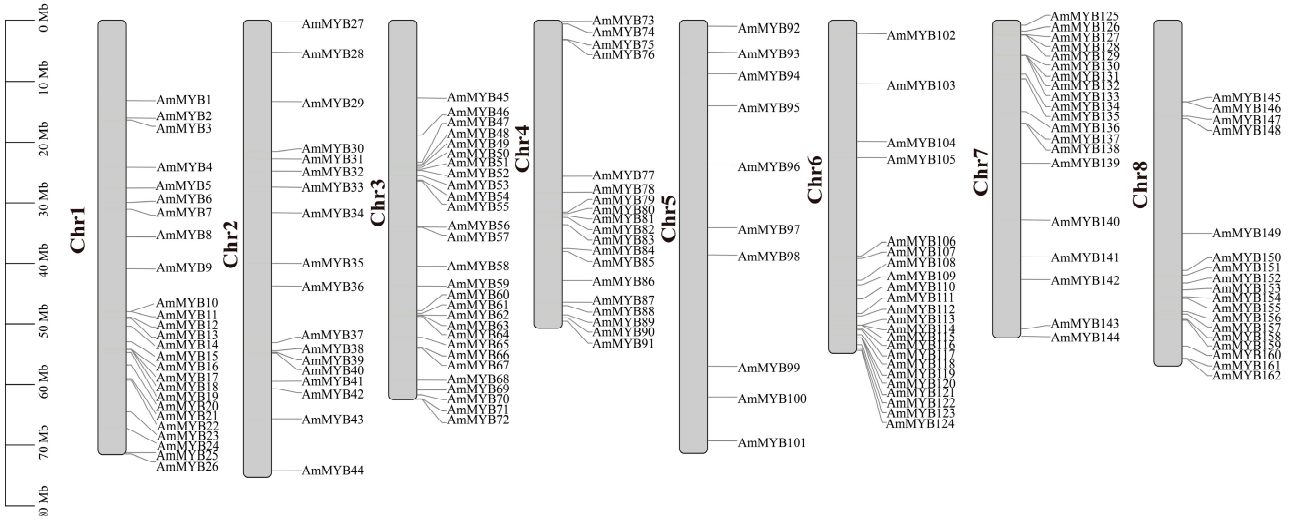


Figure 4. Chromosome localization of *MYB* gene in *A. majus*. The scale bar on the left displays the length of tobacco chromosomes.

3.5. Collinearity Analysis of A. majus

The evolution of gene families will be driven by gene replication. To further investigate the expansion relationship among members of the *AmMYB* genes family members in snapdragons, collinearity detection was employed to analyze the replication events of the *AmMYB* genes in snapdragons. As depicted in Figure 5, the *AmMYB* genes of the snapdragon showed a total of 38 repeated events, including 8 tandem repeats, located on chromosome 1 in *AmMYB16* and *AmMYB18* and *AmMYB17* and *AmMYB18*, respectively. *AmMYB113* and *AmMYB114*, *AmMYB114* and *AmMYB115* and *AmMYB119* and *AmMYB120* on chromosome 6. *AmMYB130* and *AmMYB131*, *AmMYB131* and *AmMYB132*, and *AmMYB132* and *AmMYB133* on chromosome 7. The *AmMYB* gene fragment of snapdragons appeared 30 times, distributed on chromosomes 1, 2, 4, 6 and 7. The above results indicate that the main form of amplification of the *MYB* genes family in snapdragons is fragment duplication, which plays an important role in the evolutionary process of snapdragons. To investigate the selection process of snapdragons, the ratio of non-synonymous substitution frequency (Ka) and synonymous substitution frequency (Ks) was calculated. It was found that the Ka/Ks values of the *MYB* gene tandem replication gene pairs in snapdragons were all less than 1 (Supplementary Table S5), indicating that the *MYB* replication event in snapdragons was purified and selected during the evolution process. In order to further explore the evolutionary relationship between members of the *AmMYB* genes family and different species, we selected four species: *Arabidopsis*, tomato,

potato and rice to investigate their collinearity with the *AmMYB* genes. In our study, the *AmMYB* genes have 134 homologous genes with *Arabidopsis*, 152 homologous genes in tomato (*Solanum lycopersicum*), 128 homologous genes in potato (*Solanum tuberosum*) and only 34 homologous genes in rice (*Oryza sativa*) (Figure 6, Supplementary Table S6). Overall, the *AmMYB* gene has a higher homology with dicotyledonous plants, much higher than the homologous *MYB* gene in monocotyledonous.

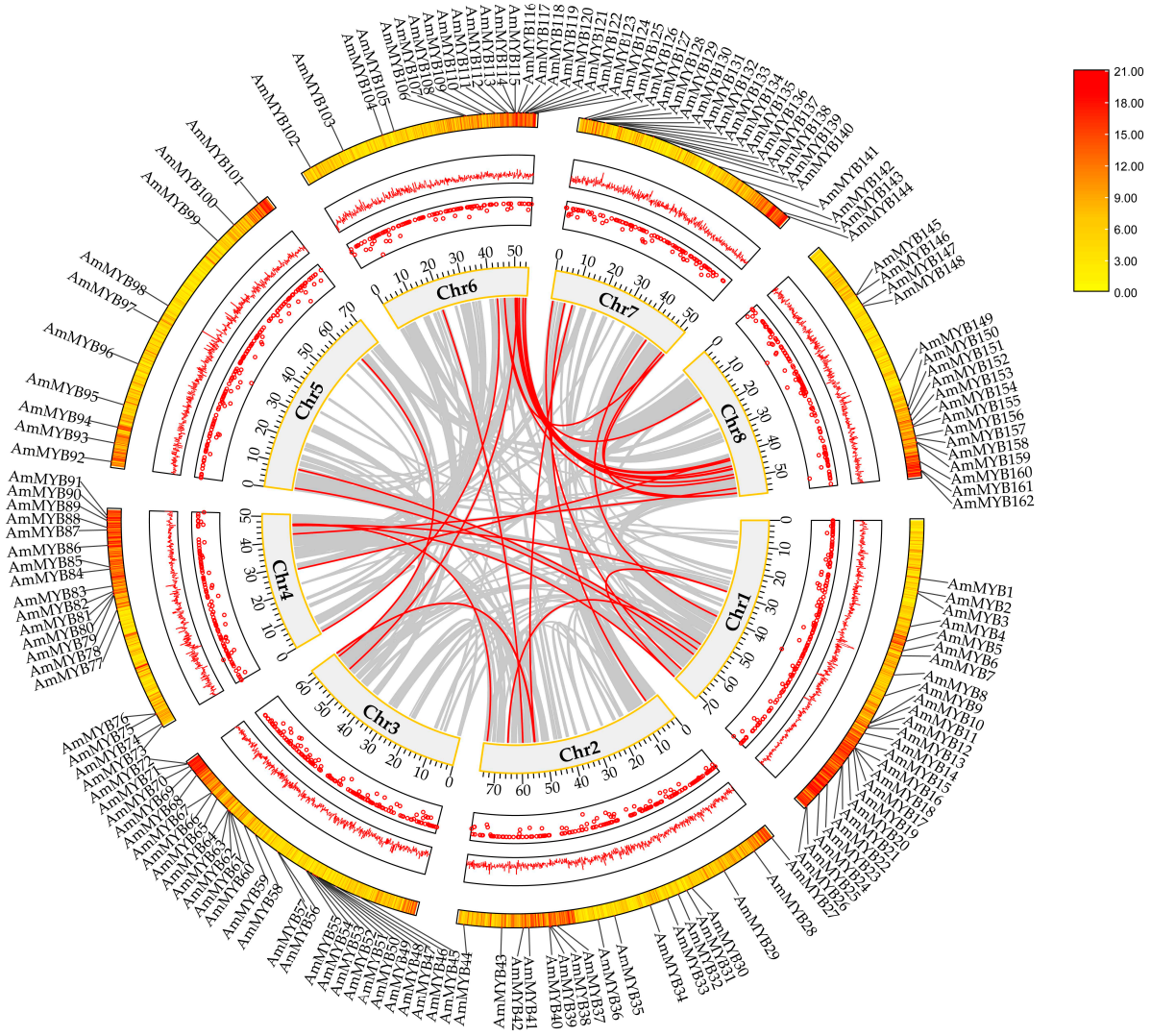


Figure 5. Collinearity of *AmMYB* genes in snapdragons. The gray line represents all collinearity of the snapdragons, and the red line represents the collinearity of the snapdragon *MYB*.

3.6. Cis-Acting Elements in the Promoter of AmMYB Genes

The cis-acting elements of the *AmMYB* genes can be categorized into 4 distinct groups, namely plant photo response elements, growth and development-related elements, stress resistance-related elements and plant hormone-related elements (Figure 7). Plant photo-responsive elements (2021/4150) are the most abundant among the four types of elements, comprising a total of 18 specific regulatory elements. Among the cis-acting elements related to plant growth and development (315/4150), a total of 11 cis-acting elements related to cell development were identified, namely circadian regulation (circadian), maize protein metabolism (O2 site), meristem expression (CAT box), cell cycle regulation (MSA like), seed-specific regulation (RY-element) and endosperm specific expression (GCN4 motif). There are also cis-acting elements at 4 protein binding sites (AT-rich element, Box III, CCAAT box, HD Zip 3), with the O2 site element accounting for the highest proportion of 22.54%. The

number of cis-acting elements (1260/4150) involved in hormone response is second only to plant photo-responsive elements, primarily consisting of abscisic acid-responsive elements (ABRE), methyl jasmonate-responsive elements (TGACG motif, CGTCA motif), salicylic acid-responsive elements (TCA element), auxin-responsive elements (AuxRR core, TGA box, TGA element) and gibberellin-responsive elements (GARE motif, TATC box, P-box). With the exception of *AmMYB22*, *AmMYB23* and *AmMYB49*, all promoters of the *AmMYB* genes contain at least one type of hormone-responsive element *MYB*. The identification of at least six stress-resistant elements (554/4150) was made, including anaerobic induction-related ARE, hypoxia-specific induction-related GC motif, low-temperature induction-related LTR, defense stress-related TC rich repeats, drought-induced MBS and flavonoid biosynthesis related MBSI. In summary, the regulation of the *AmMYB* gene involves the coordinated participation of light-responsive elements, growth and development elements, stress-resistant elements and hormone-responsive elements *MYB*.

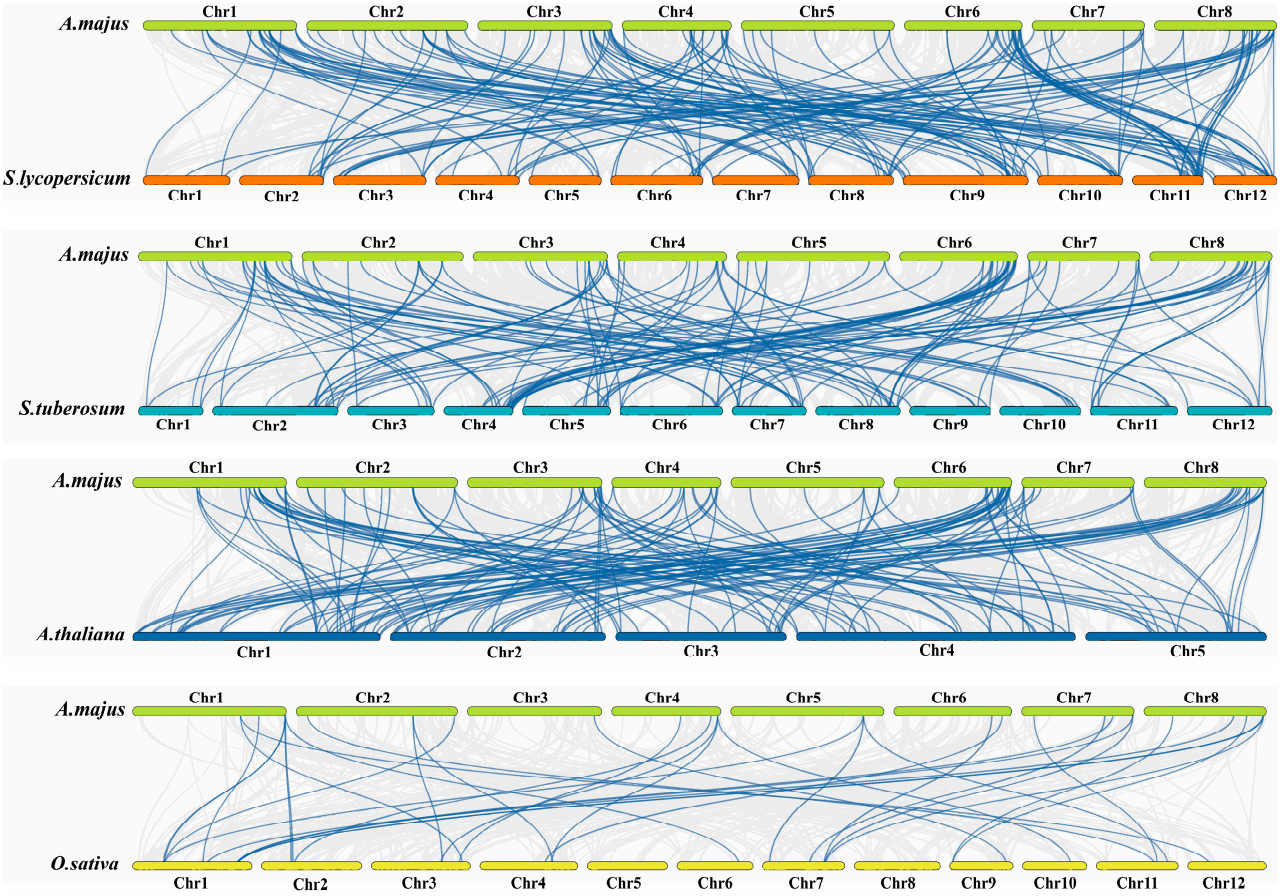


Figure 6. Collinearity analysis of *AmMYB* genes between snapdragons and 4 representative species. The gray lines indicate collinear relationships between snapdragons and other species. The blue line shows a collinear relationship with the *AmMYB* gene.

3.7. Expression Patterns of Floral Scent-Related AmMYB Genes in Snapdragons

To analyze the expression patterns of the *AmMYB* genes in different organs and flower development stages of two cultivars, we specifically selected the FPKM values from the A3 stage flower transcriptome of Am13 and Am15 for subsequent heat map analysis (Figure 8a, Supplementary Table S7). A total of 43 differentially expressed *AmMYB* genes in the A3 stage of Am13 and Am15 cultivars were found. Among them, 19 appear in the 1R subgroup, belonging to the R-R-type, I-box-binding-like, CPC-like and CCA1-like subgroups. There are a total of 23 genes belonging to the R2R3 subgroups, including A7, A5, A3, A26, A22, A2, A19, A16, A15, A14, A13 and A1 subgroups. The R1R2R3 subgroup only shows *AmMYB33* (Figure 8a).

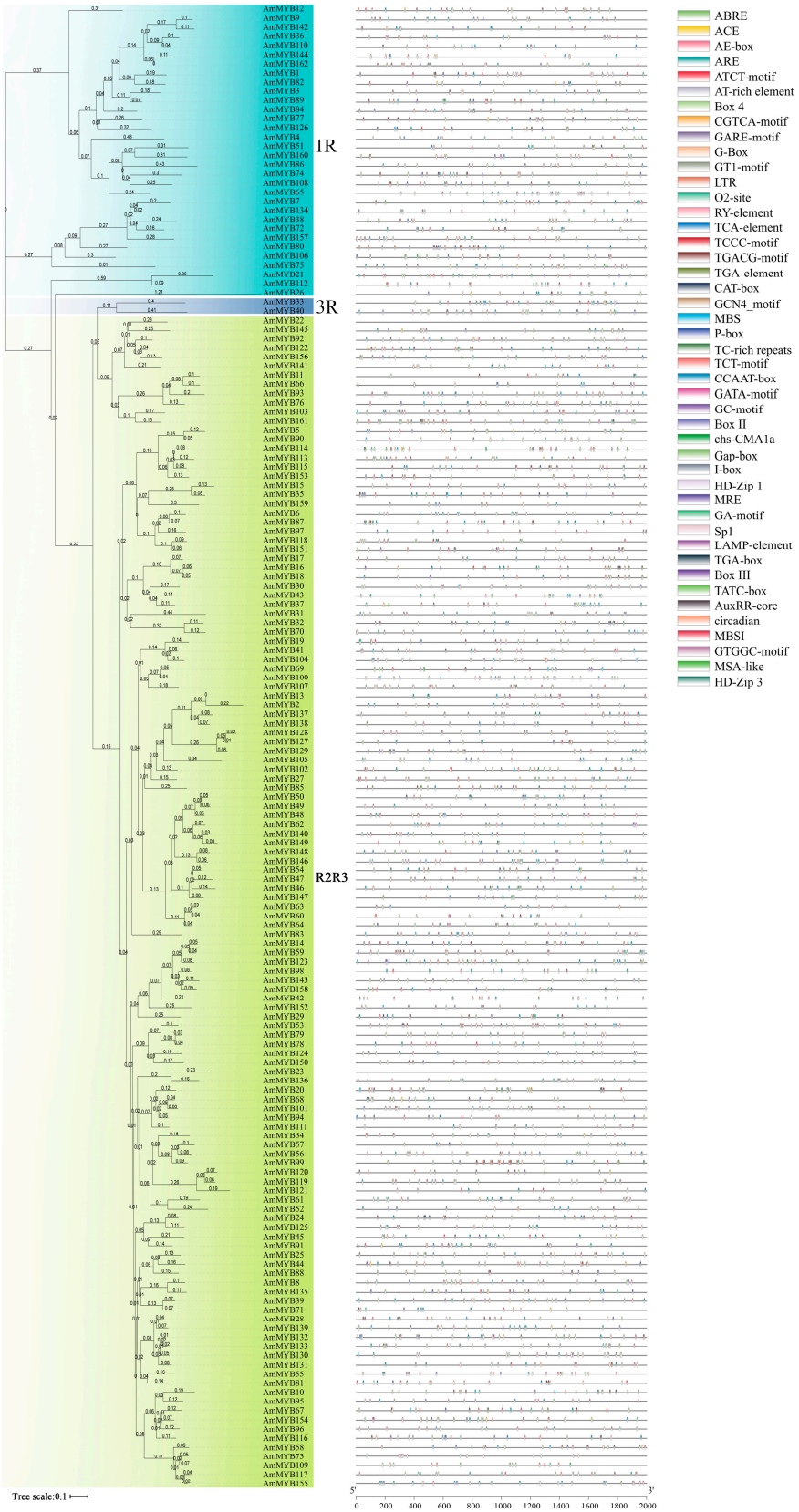


Figure 7. Cis-regulatory elements in the promoter regions of the *AmMYB* genes. Different cis-regulatory elements are represented with different colored boxes, which are placed at the top on the right. The element size is estimated by the scale at the bottom.

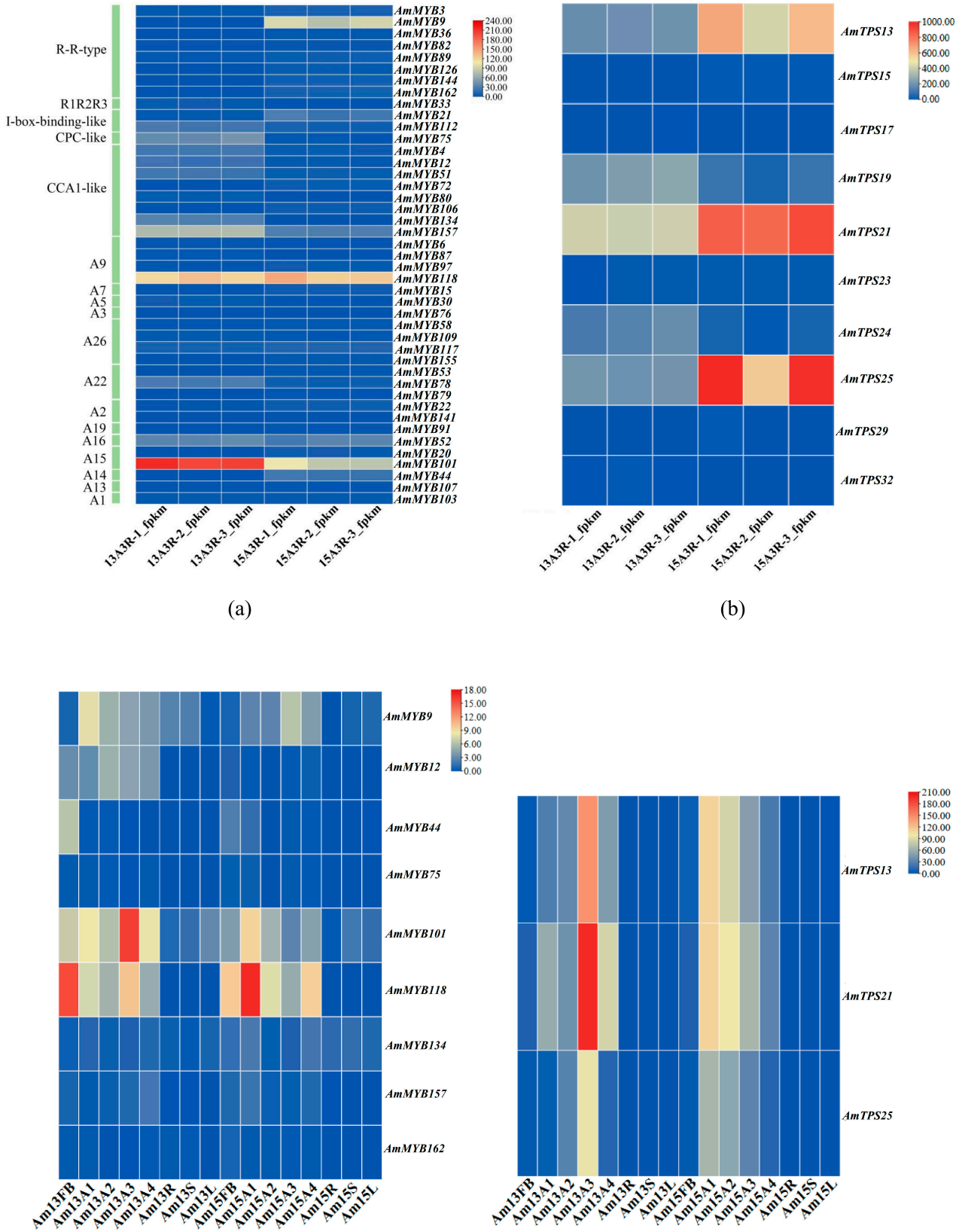


Figure 8. Gene expression heatmap. (**a**,**b**) FPKM of *AmMYB* and *AmTPS* genes during the A3 stage of Am13 and Am15 cultivars. (**c**,**d**) Expression levels of 9 *AmMYB and* 3 *AmTPSs* genes of Am13 and Am15 cultivars. (FB, A1, A2, A3, A4: different flowering stages; R: root; S: stem; L: leaf).

Additionally, it is worth noting that our metabolome data has already revealed that Am15 releases a significantly greater amount of volatile terpenes and acetophenone at this stage (unpublished data). Acetophenone belongs to the group of FVBPs. However, its biosynthesis process remains unclear and requires further investigation. In our analysis of the A3 flowering transcriptome of both Am13 and Am15 cultivars, we have identified 10 differentially expressed terpene synthase (*TPS*) genes (Figure 8b). Furthermore, based on the transcriptome heatmap analysis, we identified 9 *AmMYB* genes that exhibit significant differences or high expression levels during the A3 stage of Am13 and Am15 cultivars. Notably, the expression levels of the three genes *AmTPS13*, *AmTPS21* and *AmTPS25* were significantly different in the two cultivars (Figure 8c,d). To validate these findings, qRT-PCR was performed on the selected 9 *AmMYB* genes (Figure 8c). Interestingly, the expression levels of *AmMYB101* and *AmMYB118* at each flowering stage were much higher than those in roots, stems, and leaves. This suggests their specific expression in floral tissues across both cultivars. These findings indicate that these two genes may serve as crucial transcriptional regulatory factors contributing to notable differences in floral aroma between the two cultivars.

4. Discussion

The snapdragon has gained significant attention from both consumers and researchers alike due to its desirable ornamental characteristics, strong resistance, medicinal properties, as well as the potential utilization of its petals and seed oil for edibility [72–75]. Furthermore, the recent publication of the reference genome for two snapdragon species (*A. majus* and *A. hispanicum*) has further promoted its utilization as a model organism, particularly in addressing complex questions that are difficult to resolve using other model plants [76,77]. Currently, there is extensive validation on the role of TFs in regulating the emission of volatile compounds responsible for floral fragrance across various plant species [5]. In particular, the *MYB* TF family frequently assumes a regulatory function in modulating plant secondary metabolites [7]. In this study, the snapdragon *AmMYB* TF family was comprehensively analyzed for the first time. A total of 162 *AmMYB* genes from the whole genome data of *A. majus* were identified, and their characteristics and structures were analyzed. Moreover, AmMYB TFs potentially involved in FVOC biosynthesis were identified through the utilization of phylogenetic tree and RNA-seq data.

The *MYB* gene family exhibits significant variations in membership properties and structure, a characteristic that is also observed in snapdragons. In this study, the smallest AmMYB TF consists of only 76 amino acids, while the largest one comprises 1074 amino acids. *A. majus* is a diploid plant species (2n = 2x = 16), with 8 chromosomes per haploid set. The presence of *AmMYB* genes has been identified on each chromosome. Importantly, the abundance of the *AmMYB* genes in snapdragon genomes does not necessarily correlate with genome size or ploidy level. Compared to other plants, the number of *MYB* in *A. majus* is higher than 140 in tomatoes and 130 in rice, but lower than 198 in Arabidopsis and 719 in wheat (Supplementary Table S1). However, the 510 MB genome data of *A. majus* is much larger than that of *A. thaliana* (135 MB) [17], wheat (*Triticum aestivum*)(125 MB) [78] and rice (*O. sativa*) (398 MB) [20], and smaller than tomato (*S. lycopersicum*)(950 MB) [79], indicating that the number of *MYB* members in plants is not directly related to genome size.

Due to the extensive replication of MYB TFs during evolution, new members are involved in specific functions. *A. majus* had a whole-genome duplication (WGD) event that occurred around 46–49 Ma [76]. WGD and segmental duplicates are the main driving forces for the expansion of the *AmMYB* family in *A. majus*. The same phenomenon was also found in the study of pomegranate [80].

The promoter region of the *AmMYB* gene was found to contain a diverse array of developmental-related, light-responsive, plant hormone-responsive, and stress-responsive cis-acting elements. These cis-acting elements exhibit similarities with those identified in *MYB* genes from *A. thaliana*, *Prunus avium*, *Pyropia yezoensis* and other plant species [17,81,82]. The majority of *AmMYB* genes have a conserved exon–intron structure with minimal irreg-

ularities, likely due to intron gain, loss or stripping during the formation of the *MYB* gene family [83]. Some *AmMYB* genes consist only of exons, similar to observations in *Dianthus caryophyllus* and *Dalbergia odorifera* [17,84,85]. Evolutionary analysis suggests that these particular *MYB* genes are primitive and highly conserved throughout evolution; their functions may have undergone limited differentiation [86,87]. Most members possess 2–3 exons in the *R2R3-MYB* subfamily, consistent with studies on other species. The absence of the S5, S12 and S15 subgroups suggests their potential loss during evolutionary processes. Furthermore, notable variations among members within specific subgroups indicate functional diversification resulting from snapdragon's evolutionary trajectory [4,17,88].

Previous research findings indicate that certain MYB TFs, especially the R2R3-MYB subgroup, are involved in the biosynthesis of FVTs and FVBPs [43,50]. AtMYB21 has been identified as a key regulator for linalool synthesis in *Arabidopsis* [47]. Under the induction of blue light, AmMYB24 activates snapdragon ocimene synthase gene (*AmOCS*) by binding to the MYB COREATCYCB1 motif of *AmOCS*, resulting in the production of a large amount of terpene compounds in snapdragons [60]. Overexpression of LiMYB1 (S4), LiMYB305 (S19), and LiMYB330 (S4) in flowers increases the release of some major monoterpenes, such as linalool and ocimene, while the expression of *LiTPS2* is enhanced. In addition, LiMYB1 (S4) from the same subfamily can interact with LiMYB308 (S4) and LiMYB330 (S4), indicating their synergistic effect in regulating terpene biosynthesis [89].

In *Hedychium coronarium* flowers, HcMYB1 and HcMYB2 positively regulate the biosynthesis of methyl benzoate. Additionally, HcMYB2 can also activate the linalool synthase gene *HcTPS5*, enhancing linalool biosynthesis [51]. The snapdragon AmMYB158, AmMYB143, and AmMYB123 exhibit significant sequence similarity to HcMYB1 (Supplementary Table S8). However, the expression levels of AmMYB158, AmMYB143, and AmMYB123 in both *A. majus* (Am13 and Am15) are relatively low, suggesting that the release of benzene-related volatile compounds in the two cultivars may be relatively low [51]. Both genes showed high expression levels in Am13 and Am15. Therefore, it is hypothesized that the binding of AmMYB118 to the promoter region of *AmTPS19* positively regulates the expression of the gene, facilitating terpenoid synthesis [51].

So far, a MYB transcription factor belonging to the 1R subgroup, AmLHY, has been found to be functional in both FVTs and FVPBs biosynthesis. Knocking out AmLHY in snapdragons affects their growth and release of FVOCs, including acetophenone, methyl benzoate, 3,5-dimethyltoluene, ocimene, and linalool among other substances [62].

5. Conclusions

This study identified 162 members of the AmMYB TFs from the *A. majus* genome and conducted bioinformatics analyses to unveil their characteristics. The results showed that the AmMYB TFs were distributed on 8 chromosomes, with amino acid lengths ranging from 76–1074 aa and protein molecular weights ranging from 8.65 kDa to 119.64 kDa for each member. Most members were located in the nucleus. They are divided into three subfamilies on the phylogenetic tree, namely 1R-AmMYB, R2R3-AmMYB and 3R-AmMYB. In addition, we screened AmMYB TF members who may be involved in regulating the biosynthesis of volatile organic compounds in snapdragon fragrance through transcriptome analysis and predicted the relationship between these family members and genes related to FVOC synthesis. This study provides valuable insights for further research on AmMYB TFs and FVOC synthesis.

Supplementary Materials: The following supporting information can be downloaded at: https://www.mdpi.com/article/10.3390/horticulturae10020136/s1.

Author Contributions: Conceptualization, Z.Q. and L.C.; methodology, X.S.; software, S.S.; validation, X.S. and S.S.; formal analysis, Y.K.; investigation, Z.Q. and L.C.; resources, Z.Q. and L.C.; data curation, X.S. and S.S.; writing—original draft preparation, X.S. and S.S.; writing—review and editing, S.D. and F.W.; visualization, S.D. and C.M.; supervision, Z.Q. and L.C.; project administration, Z.Q. and

L.C.; funding acquisition, Z.Q. and L.C. All authors have read and agreed to the published version of the manuscript.

Funding: This research was funded by the Natural Science Foundation of China, grant number 32360419 and the Fundamental Research Program of Yunnan Province, grant number 202001AS070039.

Data Availability Statement: Data supporting reported results can be requested by contacting the corresponding author. The data are not publicly available due to compliance with data protection regulations.

Conflicts of Interest: The authors declare no conflicts of interest.

References

1. Wang, Z.; Tang, J.; Hu, R.; Wu, P.; Hou, X.L.; Song, X.M.; Xiong, A.S. Genome-wide analysis of the R2R3-MYB transcription factor genes in *Chinese cabbage* (*Brassica rapa* ssp. pekinensis) reveals their stress and hormone responsive patterns. *BMC Genom.* **2015**, *16*, 17. [CrossRef]
2. Ptashne, M. How eukaryotic transcriptional activators work. *Nature* **1988**, *335*, 683–689. [CrossRef]
3. Abbas, F.; Ke, Y.; Zhou, Y.; Yu, Y.; Waseem, M.; Ashraf, U.; Wang, C.; Wang, X.; Li, X.; Yue, Y.; et al. Genome-wide analysis reveals the potential role of myb transcription factors in floral scent formation in *Hedychium coronarium*. *Front. Plant Sci.* **2021**, *12*, 623742. [CrossRef] [PubMed]
4. Dubos, C.; Stracke, R.; Grotewold, E.; Weisshaar, B.; Martin, C.; Lepiniec, L. MYB transcription factors in *Arabidopsis*. *Trends Plant Sci.* **2010**, *15*, 573–581. [CrossRef] [PubMed]
5. McCarthy, R.L.; Zhong, R.; Fowler, S.; Lyskowski, D.; Piyasena, H.; Carleton, K.; Spicer, C.; Ye, Z.H. The poplar MYB transcription factors, PtrMYB3 and PtrMYB20, are involved in the regulation of secondary wall biosynthesis. *Plant Cell Physiol.* **2010**, *51*, 1084–1090. [CrossRef] [PubMed]
6. Medina-Puche, L.; Cumplido-Laso, G.; Amil-Ruiz, F.; Hoffmann, T.; Ring, L.; Rodríguez-Franco, A.; Caballero, J.L.; Schwab, W.; Muñoz-Blanco, J.; Blanco-Portales, R. MYB10 plays a major role in the regulation of flavonoid/phenylpropanoid metabolism during ripening of *Fragaria* x *ananassa* fruits. *J. Exp. Bot.* **2014**, *65*, 401–417. [CrossRef] [PubMed]
7. Tuan, P.A.; Bai, S.; Yaegaki, H.; Tamura, T.; Hihara, S.; Moriguchi, T.; Oda, K. The crucial role of PpMYB10.1 in anthocyanin accumulation in peach and relationships between its allelic type and skin color phenotype. *BMC Plant Biol.* **2015**, *15*, 280. [CrossRef]
8. Kranz, H.; Scholz, K.; Weisshaar, B. c-MYB oncogene-like genes encoding three MYB repeats occur in all major plant lineages. *Plant J.* **2000**, *21*, 231–235. [CrossRef]
9. Liu, D.; Gu, C.; Fu, Z.; Wang, Z. Genome-wide identification and analysis of MYB transcription factor family in *Hibiscus hamabo*. *Plants* **2023**, *12*, 1429. [CrossRef]
10. Wang, J.; Liu, Y.; Tang, B.; Dai, X.; Xie, L.; Liu, F.; Zou, X. Genome-wide identification and capsaicinoid biosynthesis-related expression analysis of the R2R3-MYB gene family in *Capsicum annuum* L. *Front. Genet.* **2020**, *11*, 598183. [CrossRef]
11. Arce-Rodríguez, M.L.; Martínez, O.; Ochoa-Alejo, N. Genome-wide identification and analysis of the MYB transcription factor gene family in Chili Pepper (*Capsicum* spp.). *Int. J. Mol. Sci.* **2021**, *22*, 2229. [CrossRef]
12. Wang, Y.; Zhang, Y.; Fan, C.; Wei, Y.; Meng, J.; Li, Z.; Zhong, C. Genome-wide analysis of MYB transcription factors and their responses to salt stress in *Casuarina equisetifolia*. *BMC Plant Biol.* **2021**, *21*, 328. [CrossRef]
13. Ogata, K.; Morikawa, S.; Nakamura, H.; Hojo, H.; Yoshimura, S.; Zhang, R.; Aimoto, S.; Ametani, Y.; Hirata, Z.; Sarai, A.; et al. Comparison of the free and DNA-complexed forms of the DNA-binding domain from c-MYB. *Nat. Struct. Biol.* **1995**, *2*, 309–320. [CrossRef]
14. Ogata, K.; Kanei-Ishii, C.; Sasaki, M.; Hatanaka, H.; Nagadoi, A.; Enari, M.; Nakamura, H.; Nishimura, Y.; Ishii, S.; Sarai, A. The cavity in the hydrophobic core of MYB DNA-binding domain is reserved for DNA recognition and trans-activation. *Nat. Struct. Biol.* **1996**, *3*, 178–187. [CrossRef] [PubMed]
15. Xu, W.; Dubos, C.; Lepiniec, L. Transcriptional control of flavonoid biosynthesis by MYB-bHLH-WDR complexes. *Trends Plant Sci.* **2015**, *20*, 176–185. [CrossRef] [PubMed]
16. Hichri, I.; Barrieu, F.; Bogs, J.; Kappel, C.; Delrot, S.; Lauvergeat, V. Recent advances in the transcriptional regulation of the flavonoid biosynthetic pathway. *J. Exp. Bot.* **2011**, *62*, 2465–2483. [CrossRef]
17. Stracke, R.; Werber, M.; Weisshaar, B. The R2R3-MYB gene family in *Arabidopsis thaliana*. *Curr. Opin. Plant Biol.* **2001**, *4*, 447–456. [CrossRef] [PubMed]
18. Ramalingam, A.; Kudapa, H.; Pazhamala, L.T.; Garg, V.; Varshney, R.K. Gene expression and yeast two-hybrid studies of 1R-MYB transcription factor mediating drought stress response in chickpea (*Cicer arietinum* L.). *Front. Plant Sci.* **2015**, *6*, 1117. [CrossRef]
19. Shen, X.J.; Wang, Y.Y.; Zhang, Y.X.; Guo, W.; Jiao, Y.Q.; Zhou, X.A. Overexpression of the wild soybean R2R3-MYB transcription factor GsMYB15 enhances resistance to salt stress and helicoverpa armigera in transgenic *Arabidopsis*. *Int. J. Mol. Sci.* **2018**, *19*, 3958. [CrossRef]

20. Chen, Y.; Yang, X.; He, K.; Liu, M.; Li, J.; Gao, Z.; Lin, Z.; Zhang, Y.; Wang, X.; Qiu, X.; et al. The MYB transcription factor superfamily of *Arabidopsis*: Expression analysis and phylogenetic comparison with the rice MYB family. *Plant Mol. Biol.* **2006**, *60*, 107–124. [CrossRef]
21. Schaffer, R.; Ramsay, N.; Samach, A.; Corden, S.; Putterill, J.; Carré, I.A.; Coupland, G. The late elongated hypocotyl mutation of *Arabidopsis* disrupts circadian rhythms and the photoperiodic control of flowering. *Cell* **1998**, *93*, 1219–1229. [CrossRef]
22. Wang, Z.Y.; Tobin, E.M. Constitutive expression of the *CIRCADIAN CLOCK ASSOCIATED 1* (*CCA1*) gene disrupts circadian rhythms and suppresses its own expression. *Cell* **1998**, *93*, 1207–1217. [CrossRef]
23. Kirik, V.; Simon, M.; Huelskamp, M.; Schiefelbein, J. The *ENHANCER OF TRY AND CPC1* gene acts redundantly with *TRIPTYCHON* and *CAPRICE* in trichome and root hair cell patterning in *Arabidopsis*. *Dev. Biol.* **2004**, *268*, 506–513. [CrossRef]
24. Lee, M.M.; Schiefelbein, J. Cell pattern in the *Arabidopsis* root epidermis determined by lateral inhibition with feedback. *Plant Cell* **2002**, *14*, 611–618. [CrossRef]
25. Rosinski, J.A.; Atchley, W.R. Molecular evolution of the MYB family of transcription factors: Evidence for polyphyletic origin. *J. Mol. Evol.* **1998**, *46*, 74–83. [CrossRef] [PubMed]
26. Wei, Q.; Chen, R.; Wei, X.; Liu, Y.; Zhao, S.; Yin, X.; Xie, T. Genome-wide identification of R2R3-MYB family in wheat and functional characteristics of the abiotic stress responsive gene TaMYB344. *BMC Genom.* **2020**, *21*, 792. [CrossRef] [PubMed]
27. Liu, J.; Osbourn, A.; Ma, P. MYB Transcription factors as regulators of phenylpropanoid metabolism in plants. *Mol. Plant* **2015**, *8*, 689–708. [CrossRef] [PubMed]
28. Nesi, N.; Jond, C.; Debeaujon, I.; Caboche, M.; Lepiniec, L. The *Arabidopsis TT2* gene encodes an R2R3 MYB domain protein that acts as a key determinant for proanthocyanidin accumulation in developing seed. *Plant Cell* **2001**, *13*, 2099–2114. [CrossRef] [PubMed]
29. Schaart, J.G.; Dubos, C.; Romero De La Fuente, I.; van Houwelingen, A.; de Vos, R.C.H.; Jonker, H.H.; Xu, W.; Routaboul, J.M.; Lepiniec, L.; Bovy, A.G. Identification and characterization of MYB-bHLH-WD40 regulatory complexes controlling proanthocyanidin biosynthesis in strawberry (*Fragaria* × *ananassa*) fruits. *New Phytol.* **2013**, *197*, 454–467. [CrossRef] [PubMed]
30. Terrier, N.; Torregrosa, L.; Ageorges, A.; Vialet, S.; Verriès, C.; Cheynier, V.; Romieu, C. Ectopic expression of VvMYBPA2 promotes proanthocyanidin biosynthesis in grapevine and suggests additional targets in the pathway. *Plant Physiol.* **2009**, *149*, 1028–1041. [CrossRef]
31. Wang, Y.; Liu, W.; Jiang, H.; Mao, Z.; Wang, N.; Jiang, S.; Xu, H.; Yang, G.; Zhang, Z.; Chen, X. The R2R3-MYB transcription factor MdMYB24-like is involved in methyl jasmonate-induced anthocyanin biosynthesis in apple. *Plant Physiol. Biochem.* **2019**, *139*, 273–282. [CrossRef]
32. Wan, S.; Li, C.; Ma, X.; Luo, K. PtrMYB57 contributes to the negative regulation of anthocyanin and proanthocyanidin biosynthesis in poplar. *Plant Cell Rep.* **2017**, *36*, 1263–1276. [CrossRef]
33. Li, Z.; Li, J.; Ye, X.; Zheng, X.; Tan, B.; Li, J.; Cheng, J.; Wang, W.; Zhang, L.; Wang, X.; et al. VvERF95 regulates chlorophyll degradation by transcriptional activation of VvPAO1 causing grape rachis degreening after harvesting. *Sci. Hortic.* **2022**, *303*, 111224. [CrossRef]
34. Dubos, C.; Le Gourrierec, J.; Baudry, A.; Huep, G.; Lanet, E.; Debeaujon, I.; Routaboul, J.M.; Alboresi, A.; Weisshaar, B.; Lepiniec, L. MYBL2 is a new regulator of flavonoid biosynthesis in *Arabidopsis thaliana*. *Plant J.* **2008**, *55*, 940–953. [CrossRef]
35. Yan, J.; Wang, B.; Zhong, Y.; Yao, L.; Cheng, L.; Wu, T. The soybean R2R3 MYB transcription factor GmMYB100 negatively regulates plant flavonoid biosynthesis. *Plant Mol. Biol.* **2015**, *89*, 35–48. [CrossRef] [PubMed]
36. Pérez-Díaz, J.R.; Pérez-Díaz, J.; Madrid-Espinoza, J.; González-Villanueva, E.; Moreno, Y.; Ruiz-Lara, S. New member of the R2R3-MYB transcription factors family in grapevine suppresses the anthocyanin accumulation in the flowers of transgenic tobacco. *Plant Mol. Biol.* **2016**, *90*, 63–76. [CrossRef]
37. Vimolmangkang, S.; Han, Y.; Wei, G.; Korban, S.S. An apple MYB transcription factor, MdMYB3, is involved in regulation of anthocyanin biosynthesis and flower development. *BMC Plant Biol.* **2013**, *13*, 176. [CrossRef]
38. Bozzo, G.G.; Unterlander, N. In through the out door: Biochemical mechanisms affecting flavonoid glycoside catabolism in plants. *Plant Sci.* **2021**, *308*, 110904. [CrossRef]
39. Meng, Y.; Wang, Z.; Wang, Y.; Wang, C.; Zhu, B.; Liu, H.; Ji, W.; Wen, J.; Chu, C.; Tadege, M.; et al. The MYB activator WHITE PETAL1 associates with MtTT8 and MtWD40-1 to regulate carotenoid-derived flower pigmentation in medicago truncatula. *Plant Cell* **2019**, *31*, 2751–2767. [CrossRef]
40. Jiang, L.; Yue, M.; Liu, Y.; Zhang, N.; Lin, Y.; Zhang, Y.; Wang, Y.; Li, M.; Luo, Y.; Zhang, Y.; et al. A novel R2R3-MYB transcription factor FaMYB5 positively regulates anthocyanin and proanthocyanidin biosynthesis in cultivated strawberries (*Fragaria* × *ananassa*). *Plant Biotechnol. J.* **2023**, *21*, 1140–1158. [CrossRef]
41. Colquhoun, T.A.; Kim, J.Y.; Wedde, A.E.; Levin, L.A.; Schmitt, K.C.; Schuurink, R.C.; Clark, D.G. PhMYB4 fine-tunes the floral volatile signature of *Petunia x hybrida* through PhC4H. *J. Exp. Bot.* **2011**, *62*, 1133–1143. [CrossRef] [PubMed]
42. Verdonk, J.C.; Haring, M.A.; van Tunen, A.J.; Schuurink, R.C. ODORANT1 regulates fragrance biosynthesis in petunia flowers. *Plant Cell* **2005**, *17*, 1612–1624. [CrossRef] [PubMed]
43. Spitzer-Rimon, B.; Farhi, M.; Albo, B.; Cna'ani, A.; Ben Zvi, M.M.; Masci, T.; Edelbaum, O.; Yu, Y.; Shklarman, E.; Ovadis, M.; et al. The R2R3-MYB-like regulatory factor EOBI, acting downstream of EOBII, regulates scent production by activating ODO1 and structural scent-related genes in petunia. *Plant Cell* **2012**, *24*, 5089–5105. [CrossRef] [PubMed]

44. Fenske, M.P.; Hewett Hazelton, K.D.; Hempton, A.K.; Shim, J.S.; Yamamoto, B.M.; Riffell, J.A.; Imaizumi, T. Circadian clock gene *LATE ELONGATED HYPOCOTYL* directly regulates the timing of floral scent emission in *Petunia*. *Proc. Natl. Acad. Sci. USA* **2015**, *112*, 9775–9780. [CrossRef] [PubMed]
45. Medina-Puche, L.; Molina-Hidalgo, F.J.; Boersma, M.; Schuurink, R.C.; López-Vidriero, I.; Solano, R.; Franco-Zorrilla, J.M.; Caballero, J.L.; Blanco-Portales, R.; Muñoz-Blanco, J. An R2R3-MYB transcription factor regulates eugenol production in ripe strawberry fruit receptacles. *Plant Physiol.* **2015**, *168*, 598–614. [CrossRef]
46. Zhang, S.; Ma, P.; Yang, D.; Li, W.; Liang, Z.; Liu, Y.; Liu, F. Cloning and characterization of a putative R2R3 MYB transcriptional repressor of the rosmarinic acid biosynthetic pathway from *Salvia miltiorrhiza*. *PLoS ONE* **2013**, *8*, e73259. [CrossRef]
47. Yang, Z.; Li, Y.; Gao, F.; Jin, W.; Li, S.; Kimani, S.; Yang, S.; Bao, T.; Gao, X.; Wang, L. MYB21 interacts with MYC2 to control the expression of terpene synthase genes in flowers of *Freesia hybrida* and *Arabidopsis thaliana*. *J. Exp. Bot.* **2020**, *71*, 4140–4158. [CrossRef] [PubMed]
48. Reddy, V.A.; Wang, Q.; Dhar, N.; Kumar, N.; Venkatesh, P.N.; Rajan, C.; Panicker, D.; Sridhar, V.; Mao, H.Z.; Sarojam, R. Spearmint R2R3-MYB transcription factor MsMYB negatively regulates monoterpene production and suppresses the expression of geranyl diphosphate synthase large subunit (MsGPPS.LSU). *Plant Biotechnol. J.* **2017**, *15*, 1105–1119. [CrossRef]
49. Zhao, Y.; Chen, Y.; Gao, M.; Wang, Y. Alcohol dehydrogenases regulated by a MYB44 transcription factor underlie Lauraceae citral biosynthesis. *Plant Physiol.* 2023; *Online Ahead of Print*. [CrossRef]
50. Abbas, F.; Ke, Y.; Zhou, Y.; Yu, Y.; Waseem, M.; Ashraf, U.; Li, X.; Yu, R.; Fan, Y. Genome-wide analysis of ARF transcription factors reveals HcARF5 expression profile associated with the biosynthesis of β-ocimene synthase in *Hedychium coronarium*. *Plant Cell Rep.* **2021**, *40*, 1269–1284. [CrossRef]
51. Ke, Y.; Abbas, F.; Zhou, Y.; Yu, R.; Fan, Y. Auxin-responsive R2R3-MYB transcription factors HcMYB1 and HcMYB2 activate volatile biosynthesis in *Hedychium coronarium* Flowers. *Front. Plant Sci.* **2021**, *12*, 710826. [CrossRef]
52. Naing, A.H.; Soe, M.T.; Yeum, J.H.; Kim, C.K. Ethylene acts as a negative regulator of the stem-bending mechanism of different cut snapdragon cultivars. *Front. Plant Sci.* **2021**, *12*, 745038. [CrossRef]
53. Weiss, J.; Mühlemann, J.K.; Ruiz-Hernández, V.; Dudareva, N.; Egea-Cortines, M. Phenotypic space and variation of floral scent profiles during late flower development in *Antirrhinum*. *Front. Plant Sci.* **2016**, *7*, 1903. [CrossRef]
54. Pichersky, E.; Gershenzon, J. The formation and function of plant volatiles: Perfumes for pollinator attraction and defense. *Curr. Opin. Plant Biol.* **2002**, *5*, 237–243. [CrossRef] [PubMed]
55. Kolosova, N.; Sherman, D.; Karlson, D.; Dudareva, N. Cellular and subcellular localization of S-adenosyl-L-methionine:benzoic acid carboxyl methyltransferase, the enzyme responsible for biosynthesis of the volatile ester methylbenzoate in snapdragon flowers. *Plant Physiol.* **2001**, *126*, 956–964. [CrossRef]
56. Dudareva, N.; Klempien, A.; Muhlemann, J.K.; Kaplan, I. Biosynthesis, function and metabolic engineering of plant volatile organic compounds. *New Phytol.* **2013**, *198*, 16–32. [CrossRef]
57. Terry, M.I.; Carrera-Alesina, M.; Weiss, J.; Egea-Cortines, M. Transcriptional structure of petunia clock in leaves and petals. *Genes* **2019**, *10*, 860. [CrossRef]
58. Lin, I.W.; Sosso, D.; Chen, L.Q.; Gase, K.; Kim, S.G.; Kessler, D.; Klinkenberg, P.M.; Gorder, M.K.; Hou, B.H.; Qu, X.Q.; et al. Nectar secretion requires sucrose phosphate synthases and the sugar transporter SWEET9. *Nature* **2014**, *508*, 546–549. [CrossRef]
59. Sablowski, R.W.; Moyano, E.; Culianez-Macia, F.A.; Schuch, W.; Martin, C.; Bevan, M. A flower-specific MYB protein activates transcription of phenylpropanoid biosynthetic genes. *Embo J.* **1994**, *13*, 128–137. [CrossRef]
60. Han, J.; Li, T.; Wang, X.; Zhang, X.; Bai, X.; Shao, H.; Wang, S.; Hu, Z.; Wu, J.; Leng, P. AmMYB24 regulates floral terpenoid biosynthesis induced by blue light in snapdragon flowers. *Front. Plant Sci.* **2022**, *13*, 885168. [CrossRef]
61. Tamagnone, L.; Merida, A.; Parr, A.; Mackay, S.; Culianez-Macia, F.A.; Roberts, K.; Martin, C. The AmMYB308 and AmMYB330 transcription factors from antirrhinum regulate phenylpropanoid and lignin biosynthesis in transgenic tobacco. *Plant Cell* **1998**, *10*, 135–154. [CrossRef]
62. Terry, M.I.; Pérez-Sanz, F.; Navarro, P.J.; Weiss, J.; Egea-Cortines, M. The snapdragon *LATE ELONGATED HYPOCOTYL* plays a dual role in activating floral growth and scent emission. *Cells* **2019**, *8*, 920. [CrossRef]
63. Perez-Rodriguez, M.; Jaffe, F.W.; Butelli, E.; Glover, B.J.; Martin, C. Development of three different cell types is associated with the activity of a specific MYB transcription factor in the ventral petal of *Antirrhinum majus* flowers. *Development* **2005**, *132*, 359–370. [CrossRef] [PubMed]
64. Raimundo, J.; Sobral, R.; Bailey, P.; Azevedo, H.; Galego, L.; Almeida, J.; Coen, E.; Costa, M.M. A subcellular tug of war involving three MYB-like proteins underlies a molecular antagonism in *Antirrhinum* flower asymmetry. *Plant J.* **2013**, *75*, 527–538. [CrossRef]
65. Schwinn, K.; Venail, J.; Shang, Y.; Mackay, S.; Alm, V.; Butelli, E.; Oyama, R.; Bailey, P.; Davies, K.; Martin, C. A small family of MYB-regulatory genes controls floral pigmentation intensity and patterning in the genus *Antirrhinum*. *Plant Cell* **2006**, *18*, 831–851. [CrossRef]
66. Horton, P.; Park, K.J.; Obayashi, T.; Fujita, N.; Harada, H.; Adams-Collier, C.J.; Nakai, K. WoLF PSORT: Protein localization predictor. *Nucleic Acids Res.* **2007**, *35*, W585–W587. [CrossRef]
67. Chen, C.; Chen, H.; Zhang, Y.; Thomas, H.R.; Frank, M.H.; He, Y.; Xia, R. TBtools: An integrative toolkit developed for interactive analyses of big biological data. *Mol. Plant* **2020**, *13*, 1194–1202. [CrossRef] [PubMed]
68. Kumar, S.; Stecher, G.; Li, M.; Knyaz, C.; Tamura, K. MEGA X: Molecular evolutionary genetics analysis across computing platforms. *Mol. Biol. Evol.* **2018**, *35*, 1547–1549. [CrossRef]

69. Rombauts, S.; Déhais, P.; Van Montagu, M.; Rouzé, P. PlantCARE, a plant cis-acting regulatory element database. *Nucleic Acids Res.* **1999**, *27*, 295–296. [CrossRef] [PubMed]
70. Piao, C.; Wu, J.; Cui, M.L. The combination of R2R3-MYB gene *AmRosea1* and hairy root culture is a useful tool for rapidly induction and production of anthocyanins in *Antirrhinum majus* L. *AMB Express* **2021**, *11*, 128. [CrossRef] [PubMed]
71. Vandesompele, J.; De Preter, K.; Pattyn, F.; Poppe, B.; Van Roy, N.; De Paepe, A.; Speleman, F. Accurate normalization of real-time quantitative RT-PCR data by geometric averaging of multiple internal control genes. *Genome Biol.* **2002**, *3*, Research0034.1. [CrossRef]
72. González-Barrio, R.; Periago, M.J.; Luna-Recio, C.; Garcia-Alonso, F.J.; Navarro-González, I. Chemical composition of the edible flowers, pansy (*Viola wittrockiana*) and snapdragon (*Antirrhinum majus*) as new sources of bioactive compounds. *Food Chem.* **2018**, *252*, 373–380. [CrossRef]
73. Pires, E.O., Jr.; Di Gioia, F.; Rouphael, Y.; Ferreira, I.; Caleja, C.; Barros, L.; Petropoulos, S.A. The compositional aspects of edible flowers as an emerging horticultural product. *Molecules* **2021**, *26*, 6940. [CrossRef]
74. Pires, T.C.; Barros, L.; Santos-Buelga, C.; Ferreira, I.C. Edible flowers: Emerging components in the diet. *Trends Food Sci. Technol.* **2019**, *93*, 244–258. [CrossRef]
75. Kumari, P.; Bhargava, B. Phytochemicals from edible flowers: Opening a new arena for healthy lifestyle. *J. Funct. Foods* **2021**, *78*, 104375. [CrossRef]
76. Li, M.; Zhang, D.; Gao, Q.; Luo, Y.; Zhang, H.; Ma, B.; Chen, C.; Whibley, A.; Zhang, Y.; Cao, Y.; et al. Genome structure and evolution of *Antirrhinum majus* L. *Nat. Plants* **2019**, *5*, 174–183. [CrossRef]
77. Zhu, S.; Zhang, Y.; Copsy, L.; Han, Q.; Zheng, D.; Coen, E.; Xue, Y. The snapdragon genomes reveal the evolutionary dynamics of the s-locus supergene. *Mol. Biol. Evol.* **2023**, *40*, msad080. [CrossRef] [PubMed]
78. Sukumaran, S.; Lethin, J.; Liu, X.; Pelc, J.; Zeng, P.; Hassan, S.; Aronsson, H. Genome-wide analysis of MYB transcription factors in the wheat genome and their roles in salt stress response. *Cells* **2023**, *12*, 1431. [CrossRef] [PubMed]
79. Rose, A.; Meier, I.; Wienand, U. The tomato I-box binding factor LeMYBI is a member of a novel class of MYB-like proteins. *Plant J.* **1999**, *20*, 641–652. [CrossRef]
80. Suo, H.; Zhang, X.; Hu, L.; Ni, H.; Langjia, R.; Yuan, F.; Zhang, M.; Zhang, S. Unraveling the pomegranate genome: Comprehensive analysis of R2R3-MYB transcription factors. *Horticulturae* **2023**, *9*, 779. [CrossRef]
81. Sabir, I.A.; Manzoor, M.A.; Shah, I.H.; Liu, X.; Zahid, M.S.; Jiu, S.; Wang, J.; Abdullah, M.; Zhang, C. MYB transcription factor family in sweet cherry (*Prunus avium* L.): Genome-wide investigation, evolution, structure, characterization and expression patterns. *BMC Plant Biol.* **2022**, *22*, 2. [CrossRef]
82. Yu, X.; Tang, L.; Tang, X.; Mao, Y. Genome-wide identification and analysis of MYB transcription factors in *Pyropia yezoensis*. *Plants* **2023**, *12*, 3613. [CrossRef]
83. Rogozin, I.B.; Sverdlov, A.V.; Babenko, V.N.; Koonin, E.V. Analysis of evolution of exon-intron structure of eukaryotic genes. *Brief. Bioinform.* **2005**, *6*, 118–134. [CrossRef] [PubMed]
84. Wang, X.; Zhao, S.; Zhou, R.; Liu, Y.; Guo, L.; Hu, H. Identification of *Vitis vinifera* MYB transcription factors and their response against grapevine berry inner necrosis virus. *BMC Plant Biol.* **2023**, *23*, 279. [CrossRef]
85. Mercy, I.S.; Meeley, R.B.; Nichols, S.E.; Olsen, O.A. *Zea mays ZmMybst1* cDNA, encodes a single MYB-repeat protein with the VASHAQKYF motif. *J. Exp. Bot.* **2003**, *54*, 1117–1119. [CrossRef]
86. Leng, L.; Zhang, X.; Liu, W.; Wu, Z. Genome-wide identification of the *MYB* and *bHLH* families in carnations and expression analysis at different floral development stages. *Int. J. Mol. Sci.* **2023**, *24*, 9499. [CrossRef] [PubMed]
87. Ma, R.; Luo, J.; Wang, W.; Song, T.; Fu, Y. Function of the R2R3-MYB transcription factors in *Dalbergia odorifera* and their relationship with heartwood formation. *Int. J. Mol. Sci.* **2023**, *24*, 12430. [CrossRef]
88. Qualley, A.V.; Widhalm, J.R.; Adebesin, F.; Kish, C.M.; Dudareva, N. Completion of the core β-oxidative pathway of benzoic acid biosynthesis in plants. *Proc. Natl. Acad. Sci. USA* **2012**, *109*, 16383–16388. [CrossRef]
89. Guo, Y.; Guo, Z.; Zhong, J.; Liang, Y.; Feng, Y.; Zhang, P.; Zhang, Q.; Sun, M. Positive regulatory role of R2R3 MYBs in terpene biosynthesis in *Lilium* 'Siberia'. *Hortic. Plant J.* **2023**, *9*, 1024–1038. [CrossRef]

Disclaimer/Publisher's Note: The statements, opinions and data contained in all publications are solely those of the individual author(s) and contributor(s) and not of MDPI and/or the editor(s). MDPI and/or the editor(s) disclaim responsibility for any injury to people or property resulting from any ideas, methods, instructions or products referred to in the content.